Withdrawal and Restoration of Central Vagal Afferents Within the Dorsal Vagal Complex Following Subdiaphragmatic Vagotomy

James H. Peters,[1]* Zachary R. Gallaher,[1] Vitaly Ryu,[2] and Krzysztof Czaja,[1]*

[1]Program in Neuroscience, Integrative Physiology and Neuroscience (IPN), College of Veterinary Medicine, Washington State University, Pullman, Washington 99164
[2]Natural Science Center, Department of Biology, Georgia State University, Atlanta, Georgia 30302

ABSTRACT

Vagotomy, a severing of the peripheral axons of the vagus nerve, has been extensively utilized to determine the role of vagal afferents in viscerosensory signaling. Vagotomy is also an unavoidable component of some bariatric surgeries. Although it is known that peripheral axons of the vagus nerve degenerate and then regenerate to a limited extent following vagotomy, very little is known about the response of central vagal afferents in the dorsal vagal complex to this type of damage. We tested the hypothesis that vagotomy results in the transient withdrawal of central vagal afferent terminals from their primary central target, the nucleus of the solitary tract (NTS). Sprague–Dawley rats underwent bilateral subdiaphragmatic vagotomy and were sacrificed 10, 30, or 60 days later. Plastic changes in vagal afferent fibers and synapses were investigated at the morphological and functional levels by using a combination of an anterograde tracer, synapse-specific markers, and patch-clamp electrophysiology in horizontal brain sections. Morphological data revealed that numbers of vagal afferent fibers and synapses in the NTS were significantly reduced 10 days following vagotomy and were restored to control levels by 30 days and 60 days, respectively. Electrophysiology revealed transient decreases in spontaneous glutamate release, glutamate release probability, and the number of primary afferent inputs. Our results demonstrate that subdiaphragmatic vagotomy triggers transient withdrawal and remodeling of central vagal afferent terminals in the NTS. The observed vagotomy-induced plasticity within this key feeding center of the brain may be partially responsible for the response of bariatric patients following gastric bypass surgery. J. Comp. Neurol. 521:3584-3599, 2013.

INDEXING TERMS: vagus nerve; nucleus of the solitary tract; axotomy; synaptic plasticity

Coordinated gastrointestinal function and ingestive behaviors are maintained and dependent on peripheral signals arising from abdominal viscera via primary vagal afferent neurons (Schwartz, 2006; Berthoud et al., 2011). Vagal afferents innervating abdominal organs originate from perikarya located in the nodose ganglia (NG) and terminate centrally in the nucleus of the solitary tract (NTS) via the formation of strong glutamatergic synapses onto second-order neurons (Powley et al., 1987; Furness et al., 1999). Numerous studies report that abdominal surgery compromises peripheral vagal afferent innervation (Phillips et al., 2003; Li and Owyang, 2003; Phillips and Powley, 2005; Berthoud et al., 2011). Although peripheral vagal afferents eventually regenerate after a damage (Phillips et al., 2000, 2003), the nature of injury-induced retraction and reinnervation of central vagal afferent terminals projecting to the hindbrain remains unknown.

We previously reported that capsaicin-induced damage of the NG neurons is followed by a period of synaptic plasticity in the NTS (Gallaher et al., 2011).

Grant sponsor: National Football League Charities Medical Grant (to K.C.); Grant sponsor: Washington State University New Faculty Seed Grant Program (to K.C.); Grant sponsor: National Institutes of Health; grant number: R01 DK092651 (to J.H.P.).

*CORRESPONDENCE TO: Krzysztof Czaja, D. V. M., Ph. D., Dept. of VCAPP, College of Veterinary Medicine, Washington State University, 111 Wegner Hall, Pullman, WA 99164. E-mail: czajak@vetmed.wsu.edu; or James H. Peters, Ph. D., Dept. of VCAPP, College of Veterinary Medicine, Washington State University, 266 Wegner Hall, Pullman, WA 99164. E-mail: jamespeters@vetmed.wsu.edu.

Received January 2, 2013; Revised April 19, 2013;
Accepted for publication May 23, 2013.
DOI 10.1002/cne.23374
Published online June 8, 2013 in Wiley Online Library (wileyonlinelibrary.com)

Capsaicin injury initially decreased the number of synapses within the NTS, an effect that eventually reversed to control levels, consistent with central vagal afferent terminations withdrawing and then recovering over time. It is thought that reinnervation of the peripheral targets is a key factor for restoration of central synaptic connections (Brannstrom and Kellerth, 1999). Changes in the number of synapses in the spinal cord (Brannstrom and Kellerth, 1999; White and Kocsis, 2002; Sun et al., 2006) and the hindbrain (Gallaher et al., 2011) following damage to their peripheral axons suggest that central afferents reorganize their synaptic connections with the second-order neurons after injury. Electrophysiological recordings of vagal afferent to the NTS synapses following complete unilateral cervical vagotomy demonstrated a decrease in synaptic efficacy, an effect mediated via failure to translate presynaptic action-potential invasion to vesicular glutamate release (Swartz and Weinreich, 2009). Although this finding provides functional evidence of synaptic reorganization, the extent of axonal regeneration/reinnervation over longer periods of time was not determined.

Morphological studies of primary sensory afferents demonstrate peripheral nerve damage resulting in synaptic loss at central terminals, followed by recovery over time (Brannstrom and Kellerth, 1999). This reinnervation of previously contacted central neurons is thought to result from regeneration of previously injured axons and/or by the collateral sprouting of undamaged axons (Navarro et al., 2007). However, the extent to which these newly formed synapses are functional remains unknown. In the present study we test the hypothesis that damage to the peripheral axons of the vagus will produce a temporary withdrawal and then reinnervation of central vagal afferent terminals in the NTS. We report that subdiaphragmatic vagotomy results in transient decrease and recovery in the density of vagal afferents projecting to the NTS and alters both the number and functionality of NTS synapses.

MATERIALS AND METHODS

Animals

Male Sprague–Dawley rats (6 weeks old, Simonsen Laboratories, Gilroy, CA) were individually housed in a temperature-controlled vivarium with ad libitum access to food (Harlan Teklad F6 Rodent Diet W, Madison, WI) and water. Rats were maintained under a 12-hour light/dark schedule and habituated to vivarium conditions prior to surgeries. All animal procedures were approved by the Washington State University Institutional Animal Care and Use Committee and conformed to National Institutes of Health guidelines for the use of vertebrate animals (publication 86-23, revised 1985).

Subdiaphragmatic vagotomy

The dorsal and the ventral vagal nerve trunks were carefully exposed via a ventral midline laparotomy, and 5-mm-long nerve fragments were dissected from the dorsal and the ventral trunks as previously described (Ryu et al., 2010). Sham-operated control rats underwent the same procedures, but branches of the vagus nerve were left intact. Verification of completeness of the vagotomy was performed with criteria described previously (Powley et al., 1987). Immediately following the vagotomy, rats received 1 μl injections of the retrograde tracer Fast Blue (FB; 1%; EMS-CHEMIE, Gross-Umstadt, Germany) into the wall of the stomach and the wall of the proximal duodenum. One stomach injection was made in the vicinity of the ventral gastric branch and one injection in the vicinity of the dorsal gastric branch. Vagotomies were considered complete when no FB labeling could be found in the dorsal motor nucleus of the vagus (DMN) and NG. All vagotomized animals showed no FB labeling and were therefore included in the study. All of the control rats ($n = 4$ animals per time point) revealed FB labeling in the majority of DMN and NG neurons.

Biotinylated dextran amine (BDA) injection

Ten days prior to sacrifice at either 10, 30, or 60 days following the vagotomy, rats were anesthetized with a drug cocktail containing ketamine (50 mg/kg; Ketanest, Fort Dodge Animal Health, Overland Park, KS), xylazine hydrochloride (25 mg/kg; AnaSed, Lloyd Laboratories, Shenandoah, IA), and acepromazine maleate (2 mg/kg; Vedco, St. Joseph, MO), and the left NG was exposed through a midline longitudinal skin incision in the neck. A glass micropipette (10–20-μm tip size) filled with the anterograde tracer BDA (10% in 0.1 M phosphate buffer; Molecular Probes, Eugene, OR) was inserted between the left cervical vagus and the superior laryngeal nerve and advanced into the NG. Once securely in place, 200 nl of BDA was pressure injected (Picospritzer, General Valve, Fairfield, NY) directly into the NG. Ten-day vagotomy animals received BDA injection following the vagus transection, during the same surgery. Diffusion of the tracer was visualized by adding Fast Green dye (0.1% in 0.1 M PB, Sigma-Aldrich, St. Louis, MO) into the solution. Among all sham-operated controls, 5,500 μm^2 represented the average minus 1 standard deviation in the area of BDA labeling within the solitary tract (ST) of a single coronal section at the level of the area postrema. Therefore, BDA injections were considered complete when the ST showed

sufficient labeling to cover an area greater than 5,500 μm^2. This criterion resulted in the exclusion of one animal from each recovery time following vagotomy, giving a final $n = 3$ animals per time point.

Tissue fixation and sectioning

After transcardial perfusion with 0.1 M phosphate-buffered saline (PBS; pH 7.4) followed by 4% paraformaldehyde (~4°C over 20 minutes), hindbrains were harvested, postfixed in 4% paraformaldehyde for 2 hours, and immersed overnight in 30% sucrose in PBS and 0.1% NaN_{33} (Sigma-Aldrich; pH 7.4). Hindbrains were postfixed in 4% paraformaldehyde for 2 hours and then transferred into 30% sucrose (Sigma-Aldrich) and 0.1% NaN_3. Hindbrains were sectioned at 30 μm thickness throughout the rostrocaudal extent of the NTS (between bregma −11.20 and −15.97 mm) and stained for selected antigens.

Immunohistochemistry

For immunohistochemical visualization of synapses, free-floating hindbrain sections were washed three times for 15 minutes in Tris PBS (TPBS; pH 7.4) followed by a 30-minute incubation in a blocking solution of 1% normal horse serum and 0.5% Triton X-100 in TPBS. Sections were then incubated for 24 hours in polyclonal rabbit anti-synaptophysin I antiserum in blocking solution. Subsequently, sections were incubated for 2 hours in the secondary biotinylated anti-rabbit antibody (1:200 dilution, Jackson ImmunoResearch, West Grove, PA) followed by a 4-hour incubation in ABC complex (1:1,000 dilution, Vectastain Elite Kit, Vector, Burlingame, CA). Horseradish peroxidase activity was revealed by a 5-minute incubation in diaminobenzidine (DAB; Sigma-Aldrich) and H_2O_2 in TPBS. Sections were mounted on slides, air-dried, dehydrated through graded ethanol to xylene, and then coverslipped with Permount (Fisher Scientific, Fair Lawn, NJ).

For immunofluorescence, hindbrain sections underwent three 15-minure rinses in TPBS, followed by 15 minutes in 0.1% sodium borohydride in 0.1 M PBS (pH 7.4), and 15 minutes in 0.1% Triton X-100 in TPBS. Following overnight incubation in a blocking solution of 10% normal horse serum in TPBS, sections were incubated for 24 hours in a mixture of primary antisera against polyclonal rabbit anti-synapsin-1 and monoclonal mouse anti-β-III tubulin. Subsequently, sections were incubated for 2 hours at room temperature in an appropriate mixture of secondary antibodies Alexa 488 and Alexa 555 (1:400 dilution, Invitrogen, Carlsbad, CA). For immunohistochemical controls, the primary antibody was preabsorbed with the immunizing peptide overnight at 4°C. To determine whether nonspecific staining from the secondary antibody was present, an additional control group was included in which the primary antibody was omitted and replaced by preimmune serum. Both the preabsorption and the omission abolished immunolabeling for both antisera. CY3-conjugated streptavidin was used for visualization of anterogradely transported BDA (1:200 dilution, Jackson ImmunoResearch). Sections were mounted in ProLong Gold Antifade Reagent with 4′,6-diamidino-2-phenylindole (DAPI; Molecular Probes, Eugene, OR).

Antibody characterization

The list of primary antibodies used in this study is provided in Table 1. Polyclonal anti-synaptophysin I antibody recognizes a single band at 35 kDa on western blots of rat brain samples (Wimmer et al., 2006). The specificity of the antibody has been confirmed in previous immunohistochemical studies using rodent brain tissue (Herde et al., 2010; Gazula et al., 2010). The rabbit anti-synapsin 1 polyclonal antiserum recognizes two bands of 77 and 80 kDa on western blots of mouse brain extracts, corresponding to the expected size of synapsin 1a and 1b, respectively. Previous studies using array tomography have shown a dense punctuate distribution of immunolabeling with this antibody that has a high correlation with several other markers of synaptic vesicles (Micheva et al., 2010; Soiza-Reilly and Commons, 2011).

TABLE 1.
Primary Antibodies Used in This Study

Antigen	Immunogen	Dilution	Manufacturer
Synaptophysin 1	Synthetic peptide GPQGAPTSFSNQM; amino acids 301–313 in human synaptophysin 1; coupled to keyhole limpet hemocyanin via an added N-terminal cysteine residue	1:500	Synaptic Systems (Goettingen, Germany), rabbit polyclonal, 101002
Synapsin I	Synapsin I (mixture of Ia and Ib) purified from bovine brain	1:500	Millipore (Billerica, MA), rabbit polyclonal, AB1543
β-III Tubulin	Peptide corresponding to residues 436–450 of neuronal specific β-III-tubulin	1:500	Abcam (Cambridge, MA), mouse monoclonal, ab78078

According to the manufacturer's specification, the monoclonal (2G10 clone) mouse anti-β-III tubulin antibody detects a band of approximately 50 kDa on western blots from microtubules derived from rat brain.

Quantification analysis

Images of the dorsal vagal complex were viewed and captured under 200×, 400×, or 1,000×X magnification with a Nikon 80i imaging photomicroscope (Nikon, Tokyo, Japan), equipped with a digital camera (Nikon Digital Sight DS-Qi1Mc), and appropriate filters for DAPI, Alexa 488, and Alexa 555. Captured images were evaluated with the aid of a computer and the NIS-Elements AR 3.0 Imaging software (Nikon, Tokyo, Japan).

Quantification of synapsin-I, β-III tubulin, DAPI, and BDA-labeled vagal afferents in the NTS was conducted by using Nikon Elements binary imaging analysis based on principles described by Hunter et al. (2007). For quantification of synapsin-1, β-III tubulin, and DAPI, three sections from the intermediate NTS (defined by the presence of the area postrema; approximately bregma −14.25 to −13.25) were selected for analysis. For anterogradely BDA-labeled vagal afferents, every third section beginning at the far caudal end of the NTS (bregma −15.97) to the rostral extent of the labeled afferents (bregma −11.20), was analyzed. For each section, an exposure time of 200 ms was used and the left ST, left NTS, right NTS, and area postrema (where applicable) were defined as separate regions of interest. A binary threshold was set at the mean intensity plus 2 standard deviations to separate positively labeled fibers from the background. The area of positively labeled fibers above the binary threshold was recorded for each section. For each animal, the analyzed sections were binned by calculating the average area across three serial sections. The reported values represent the group mean of these binned values, with the bregma level of the center section used to define the rostral–caudal location. The final images were deconvoluted with NIS-Elements AR 3.0 software. For tpreparation of the microscopic illustrations, we used Adobe (San Jose, CA) Photoshop CS2 to adjust only the brightness, contrast, and sharpness and to make composite plates.

Synaptophysin counts within the NTS were performed at high magnification with a 100× (1.30 NA) oil objective using a Nikon 80i imaging photomicroscope equipped with Stereologer CP Version 2 Software (Stereologer Resource Center, Chester, MD). The optical fractionator was employed to obtain estimates of the total number of synaptophysin-immunoreactive (IR) synapses within the region of the NTS by using the following formula: $N = \Sigma Q - (h/t \times 1/asf \times 1/ssf)$, where ΣQ equals the total number of objects counted for each subject; *h* equals the height of the disector; *t* equals the thickness of the section; *asf* equals the area sampling fraction; and *ssf* equals the section sampling fraction (Calhoun et al., 1996).

In vitro electrophysiology

Horizontal brainstem slices

Brainstem slices were prepared from isoflurane anesthetized rats as previously described (Doyle et al., 2004). Following sacrifice, the medulla was removed and placed in cooled artificial cerebrospinal fluid (aCSF) containing (mM): 125 NaCl, 3 KCl, 1.2 KH_2PO_4, 1.2 $MgSO_4$, 25 $NaHCO_3$, 10 dextrose, and 2 $CaCl_2$, bubbled with 95% O_2/5% CO_2. The brain was trimmed to yield a tissue block centered on obex. A wedge of tissue was removed from the ventral surface so that a horizontal cut yielded a 250-μm-thick slice that contained the ST together with NTS neuronal cell bodies. Slices were cut with a sapphire knife (Delaware Diamond Knives, Wilmington, DE) mounted in a vibrating microtome (VT1000S; Leica Microsystems, Bannockburn, IL). Slices were secured in a perfusion chamber with a fine polyethylene mesh (Siskiyou Design Instruments, Grants Pass, OR), perfused with aCSF (300 mOsm), and constantly bubbled with 95% O_2, 5% CO_2, at 33°C.

Whole cell patch-clamp recordings

The anatomical landmarks preserved in the horizontal slices allowed targeting of neurons within the medial subnucleus of the caudal NTS. Recorded neurons were located medial to the ST and within 200 μm rostral or caudal of obex. Patch electrodes were visually guided to neurons using infrared illumination and differential interference contrast optics (DIC; 40× water immersion lens), on a Nikon E600 microscope (Nikon Instruments, Melville, NY). Recording electrodes (2.8–3.5 MΩ) were filled with a low Cl^- (10 mM, $E_{Cl} = -69$ mV) intracellular solution, containing (mM): 6 NaCl, 4 NaOH, 130 K-gluconate, 11 EGTA, 1 $CaCl_2$, 1 $MgCl_2$, 10 HEPES, 2 Na_2ATP, and 0.2 Na_2GTP. The intracellular solution was pH 7.3 and 296 mOsm. Neurons were studied under voltage clamp conditions with an Axopatch 200A amplifier (Molecular Devices, Union City, CA) and held at $V_H = -60$ mV using pipettes in open, whole-cell patch configuration. Signals were filtered at 10 kHz and sampled at 30 kHz by using p-Clamp software (version 9.0, Molecular Devices). See Table 2 for quantification of the number of animals, neurons, and afferent inputs recorded as well as the passive membrane properties.

Functional characterization of primary afferent innervation onto NTS neurons

A concentric bipolar stimulating electrode (200-μm outer tip diameter; Frederick Haer, Bowdoinham, ME)

TABLE 2.

Comparison of Passive Membrane Properties of Recorded NTS Neurons From Control and Vagotomized Animals at 10 and 60 Days Post Surgery[1]

	Day 10		Day 60	
	Control	VagX	Control	VagX
Animals (*n*)	4	4	3	4
Neurons (*n*)	9	14	9	14
Afferent inputs (*n*)	20	16	21	18
R_m (MΩ)	270.57 ± 39.07	557.80 ± 55.97	389.25 ± 105.25	501.60 ± 74.83
C_m (pF)	10.83 ± 1.13	6.90 ± 0.60	7.6 ± 0.90	9.00 ± 1.50

[1]Neurons from vagotomized animals had higher membrane resistance (R_m) and smaller membrane capacitance (C_m) than neurons from the control animals. These differences were statistically different at 10 days ($P = 0.003$ and $P = 0.01$, respectively) but not at 60 days post vagotomy ($P = 0.40$ and $P = 0.53$, respectively). Values are the mean ± SEM.

was placed on distal portions of the visible ST rostral to the recording region. This remote placement of the stimulating electrode (1–3 mm from recorded neurons) minimized activation of non-ST axons or local neurons due to the discrete current path within the bipolar electrode, as demonstrated in Bailey et al. (2008). Trains of current shocks were delivered to ST every 6 seconds (shock duration 0.1 μs) by using a Master-8 isolated programmable stimulator (A.M.P.I., Jerusalem, Israel). Responses to bursts of five shocks (20-ms intershock interval) assessed frequency-dependent amplitude depression for synchronous excitatory postsynaptic currents (EPSCs) produced from suprathreshold stimulation of the ST (ST-EPSCs). Latency was measured as the time between the ST shock artifact and the onset of the resulting EPSC. Synaptic jitter was calculated as the standard deviation of ST-EPSC latencies for 30–40 trials within each neuron. Jitters of <200 μs identify direct, monosynaptic afferent inputs (Doyle and Andresen, 2001). Stimulus-intensity protocols with incremental changes in stimulus intensity can discriminate single from multiple discrete ST afferent inputs to central NTS neurons (McDougall et al., 2009; Peters et al., 2011). ST afferent shocks distant to the recorded NTS neurons allow for the careful recruitment of multiple afferent inputs, which can be characterized based on: 1) intensity of stimulus needed for activation; 2) latency to event onset; and 3) amplitude (waveform) of the resulting EPSC. By using this analysis, we are able to determine the number and strength of primary afferents innervating recorded NTS neurons. Because C- and Aδ-fibers preferentially express the ion channel TRPV1, a subgroup of recordings was exposed to the TRPV1 agonist capsaicin (100 nM) to broadly classify the afferent fiber type innervating the NTS neuron (Peters et al., 2010).

Statistical analysis

Imaging studies

Statistical analyses were performed with SigmaStat 3.5 software (Systat Software, Chicago, IL). Either one-way or two-way ANOVA (followed by Fisher's or Bonferroni's post hoc test) was used for statistical comparisons. Significance was set at $P < 0.05$. All values are presented as means ± SEM.

In vitro synaptic responses

Electrophysiologically recorded neurons were included for analysis if they maintained an access resistance <20 MΩ and had stable holding currents (between 0 and 200 pA at $V_m = -60$ mV) throughout the recording. Digitized waveforms were analyzed by using an event detection and analysis program (MiniAnalysis, Synaptosoft, Decatur, GA), for all miniature synaptic currents and Clampfit 10 (Molecular Devices) for all ST-stimulated currents. To obtain accurate decay-time constants, amplitude, and baseline values for miniature synaptic currents, those events smaller than 10 pA and those with multiple peaks were excluded. All events > 10 pA were counted for frequency values. Decay-time constants were acquired by fitting a single exponential between the 10% and 90% peak amplitude portion of the current decay. For statistical comparisons, repeated-measure ANOVA, one-way ANOVA, Fisher's PLSD post hoc analysis, and the Kolmogorov–Smirnov (K-S) test, were used when appropriate. For analysis of spontaneous excitatory postsynaptic currents (sEPSCs) frequency and waveform parameters (decay-time constant and amplitude), we took the average across many events within a neuron and then combined them with the other recordings to determine the group data. Group data were compared by Friedman ANOVA on ranks or a one-way ANOVA each with post hoc testing against the control as appropriate using Sigma Stat statistical software (Systat Software, San Jose, CA). All data are represented as mean ± SEM with $P < 0.05$ considered statistically significant.

RESULTS

Neural tract tracing analysis of vagal afferent terminations in the NTS

Primary vagal afferent innervation of subdiaphragmatic structures predominantly terminates in the caudal

and intermediate regions of the NTS (Altschuler et al., 1989). To quantify vagal afferent fibers throughout the dorsal vagal complex, the anterograde tracer BDA was injected into the left NG in either control animals, or those previously vagotomized at set time points 10, 30, or 60 days prior (Fig. 1A–D). Binary analysis of the area of BDA-labeled vagal afferents across the caudal-to-rostral extent of the NTS revealed differences in distribution of labeled afferent terminations (Figs. 1, 2). Subdiaphragmatic vagotomy decreased total BDA labeling in the dorsal vagal complex by approximately 70% at 10 days post surgery (VagX: 205,756 ± 101,966 μm^2 vs. control: 645,699 ± 100,744 μm^2, $n = 3$ animals/group, $P < 0.05$; Figs. 1B, 2A,B), an effect that was reversed to control levels by 30 days post vagotomy (Figs. 1C,D, 2A,B). Further examination of the distinct subregions of the dorsal vagal complex revealed that BDA-labeled fibers in both the solitary tract (ST; 81,481 ± 40,645 μm^2 vs. control: 332,020 ± 61,337 μm^2, $n = 3$ animals/group, $P < 0.05$; Fig. 2C,D), and the ipsilateral NTS (95,209 ± 50,268 μm^2 vs. control: 257,663 ± 55,486 μm^2, $n = 3$ animals/group, $P < 0.05$; Fig. 2E,F) were reduced by approximately 75% and 65%, respectively. Changes in these specific areas accounted for most of the return of BDA labeling by 30 days post surgery (Fig. 2C–F), which remained at control levels 60 days post vagotomy. The quantities of BDA-labeled fibers in the contralateral NTS and area postrema (AP) were relatively small in comparison with the ipsilateral NTS and were not altered by vagotomy (data not shown).

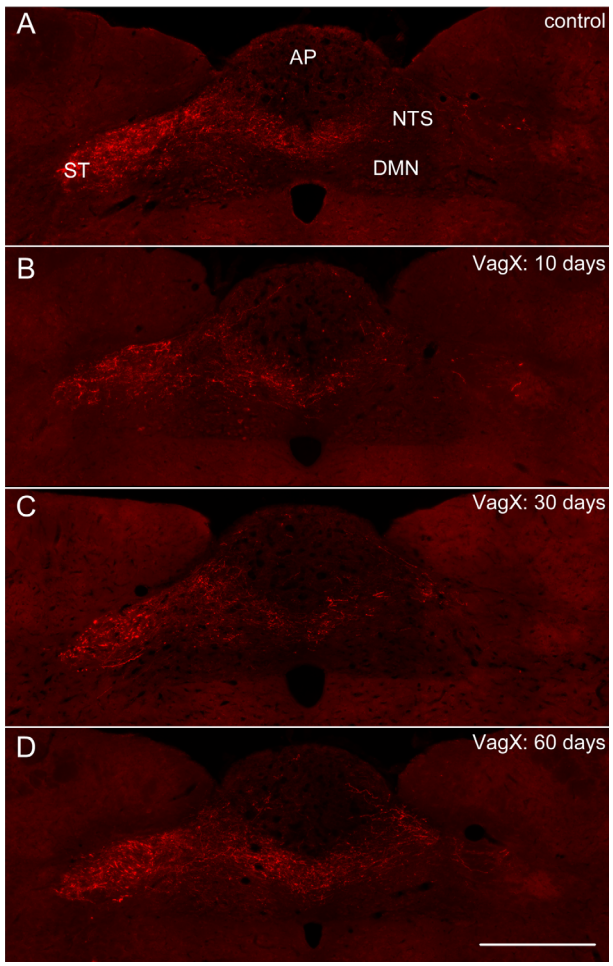

Figure 1. Subdiaphragmatic vagotomy triggers transient withdrawal of central vagal afferent fibers in the DVC. **A–D:** Representative fluorescent images of coronal sections through the dorsal vagal complex showing distribution of vagal afferent fibers anterogradely labeled with BDA injected into the left NG in control rat (A), and 10 days (B), 30 days (C), and 60 days (D) post vagotomy. Abbreviations: AP, area postrema; DMN, dorsal motor nucleus of the vagus; NTS, nucleus of the solitary tract; ST, solitary tract. Scale bar = 500 μm in D (applies to A–D).

Synaptic plasticity in the NTS following vagotomy

Central projections of vagal afferent neurons form synaptic contacts onto second-order NTS neurons (Andresen and Mendelowitz, 1996). To morphologically quantify the number of synaptic contacts in the NTS, we selectively immunostained the synapse-specific proteins synaptophysin and synapsin 1 (Figs. 3,4A,B). Stereological analysis revealed a statistically significant main effect difference in the number of synaptophysin-IR synapses in vagotomized versus control animals ($n = 6$ animals/group; Fig. 4A). Due to variability within the groups, the post hoc comparison just missed statistical significance on day 10 ($P = 0.06$; Fig. 3B). On day 30, synaptophysin immunoreactivity in the NTS of the vagotomized animals increased, but still trended lower in comparison with sham controls ($n = 6$ animals/group; Fig. 3C). On day 60, there were no differences in the numbers of synaptophysin-IR synapses in the NTS between experimental groups (Fig. 3D). Synapsin 1 (Figs. 3,4B) and β-III tubulin (Figs. 3,4C) expression in the NTS exhibited similar patterns as synaptophysin, except with much more robust statistical differences ($n = 3$ animals/group, $P < 0.01$ on day 10; $P = 0.052$ on day 30 and $P > 0.05$ on day 60). Vagotomy produced no statistically significant change in the number of NTS neurons compared with controls as quantified with the nuclear marker DAPI ($n = 3$ animals/group, $P > 0.05$, ANOVA; Fig. 4D).

The frequency of spontaneously released vesicles of glutamate provides a basic determination of the number of functional synaptic contacts onto a recorded neuron (Kavalali et al., 2011). The dominant glutamatergic input

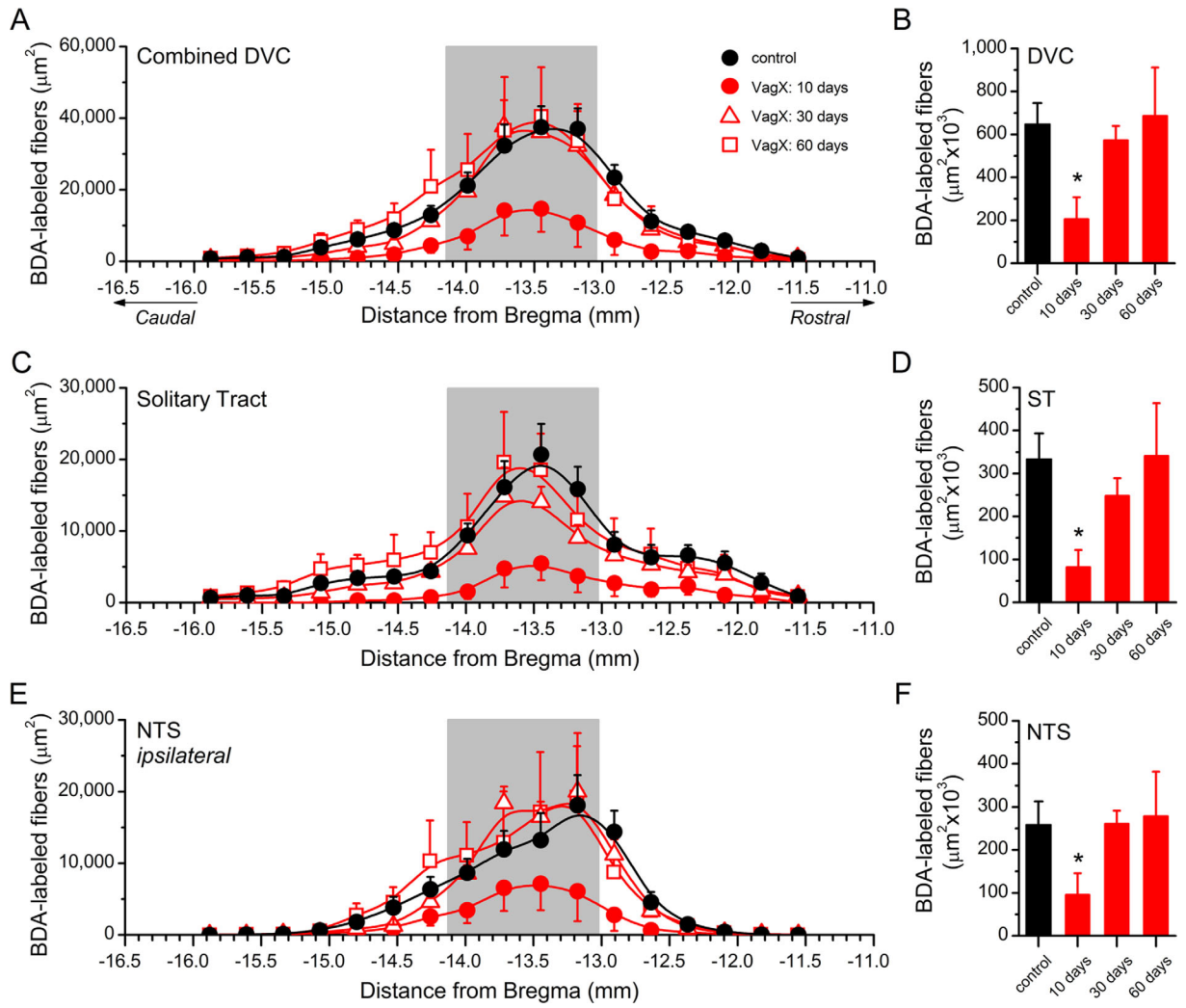

Figure 2. Quantification of fluorescence from BDA-labeled afferents. **A,B:** The caudorostral distribution of BDA-labeled afferents in the dorsal vagal complex (A) and the combined total BDA labeling (B). Area shaded in gray represents the extent of the AP. **C–F:** Selective analysis of BDA-labeled afferents in the ipsilateral ST (C,D) and ipsilateral NTS (E,F) at distinct Bregma levels (C,E), with the combined total labeling for each region in D and F. Abbreviations: NTS, nucleus of the solitary tract; ST, solitary tract. Statistical comparisons indicated are $*P < 0.05$ versus sham controls.

at medial NTS neurons is from vagal afferent innervations. Thus changes in quantal (sEPSCs) should reflect the morphological and/or functional changes in afferent innervation. In medial NTS neurons, the average frequency of sEPSCs was significantly decreased 10 days following subdiaphragmatic vagotomy (control: 10.22 ± 2.02 Hz, $n = 9$ neurons from 4 animals, vs. VagX: 3.63 ± 0.95 Hz, $n = 15$ neurons from 4 animals; $P = 0.012$); but recovered to control levels by day 60 (control: 13.87 ± 3.51 Hz, $n = 9$ neurons from 3 animals, vs. VagX: 15.63 ± 4.01 Hz, $n = 15$ neurons from 4 animals; $P = 0.74$; Fig. 5A,B). The absolute frequency of sEPSCs onto an individual neuron is relatively stable under unstimulated conditions at a constant temperature (Shoudai et al., 2010); however, across neurons there is a large degree of variability. Nonetheless, when we plot the histogram of frequencies from individual neurons, we can clearly detect a decrease in frequencies in the vagotomized group at day 10 (Fig. 5C). By day 60 the average frequency is equivalent to that of controls. However, this is a result of some neurons now receiving relatively high frequency of inputs while a significant population remains at the lowest end of the frequency scale (Fig. 5D). This may reflect differential reinnervation by the primary afferents or perhaps local sprouting of central neurons in response to the lesion and subsequent withdrawal of afferent innervation (Hu et al., 2004).

Although changes in sEPSC frequency reflect the number of functional synaptic contacts, this parameter

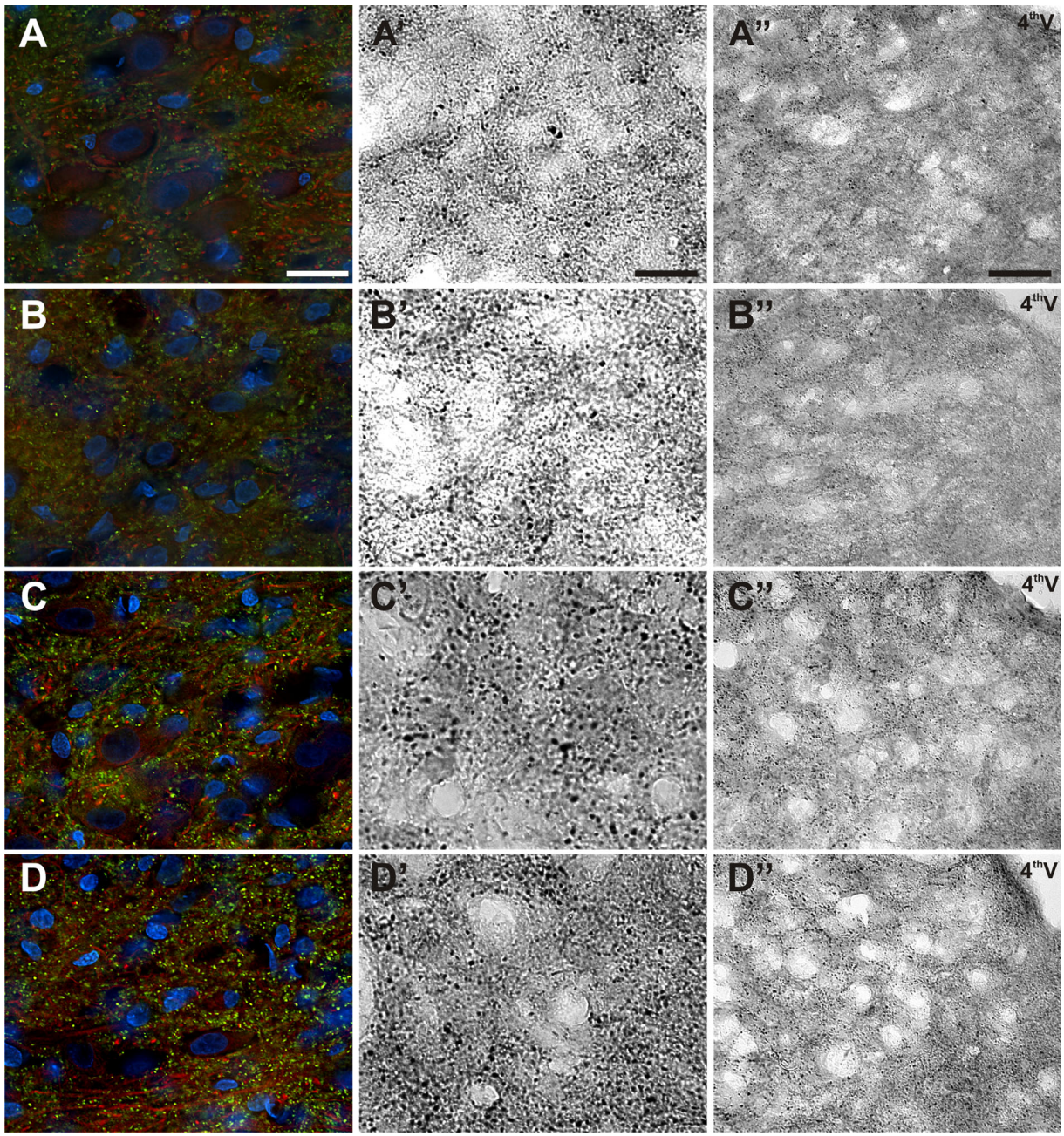

Figure 3. Subdiaphragmatic vagotomy results in synaptic loss at central terminals in the NTS, followed by recovery over time. **A–D:** Representative images of coronal sections of the NTS from control rats (A–A″) and 10 (B–B″), 30 (C–C″), and 60 days post vagotomy (D–D″). Synapsin-1–IR synapses (green), β-III tubulin–IR fibers (red) and DAPI-labeled neuronal and glia nuclei (blue) (A–D). Synaptophysin-IR synapses at high magnification (A′–D′) and low magnification (A″–″). Scale bar = 10 μm in A (applies to A–D) and A′ (applies to A′–D′); 50 μm in A″ (applies to A″–D″).

is generally considered the result of presynaptic release processes (Kavalali et al., 2011). Weakened synaptic input can also lead to changes in the distribution and number of postsynaptic specializations and receptors (Navarro, 2009). Following subdiaphragmatic vagotomy, the average sEPSC amplitude was significantly smaller at day 10 and began to recover by day 60 (Fig. 5E,F), consistent with a loss of postsynaptic receptors. In contrast, neither the rise nor the decay kinetics of sEPSCs were statistically different between control and VagX at either time point (Fig. 5G), indicating no major changes in the receptor-associated proteins mediating channel inactivation nor a dramatic shift from somatic to dendritic contacts. The histogram distributions of average sEPSC amplitudes across recorded neurons shows a concentration of smaller events 10 days

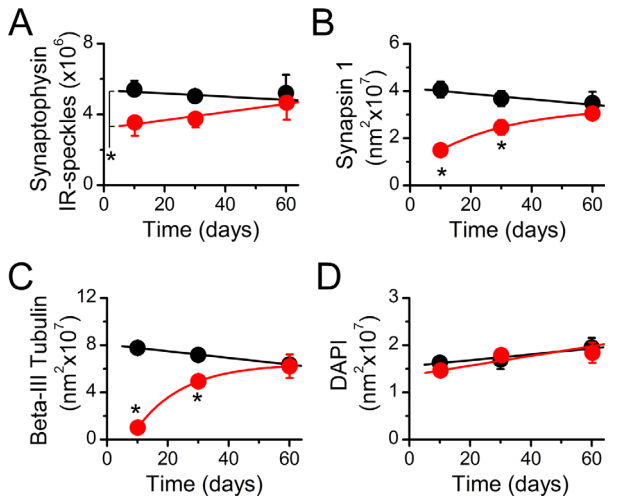

Figure 4. Quantification of immunohistochemical labeling in the NTS. **A–D:** Stereological quantification of synaptophysin (A), synapsin-1 (B), and β-III tubulin (C) revealed the loss and restoration of synapses and fibers following the vagotomy, without a change in neuronal/glia density in the NTS as shown by DAPI-labeled nuclei (D). $*P < 0.01$ versus sham controls.

following vagotomy that are redistributed more closely to control by day 60 (Fig. 5H,I).

The horizontal configuration of the brainstem slice permits selective stimulation of the ST bundle, containing the central endings of the vagus, distance (1–3 mm) to the recorded NTS neuron (Doyle and Andresen, 2001). By using a concentric bipolar stimulating electrode and graded stimulus intensity, we are able to discretely recruit individual and multiple convergent afferent inputs onto second-order NTS (McDougall et al., 2009; Peters et al., 2011). Initially, we analyzed single ST-evoked afferent inputs recruited first using the stimulus-intensity recruitment protocol (Fig. 6). The average amplitude of the ST-evoked EPSC from individual afferent inputs was significantly reduced 10 days following vagotomy but returned to control level by day 60 (Fig. 6A,B). ST-evoked EPSCs result from the simultaneous release of multiple glutamate vesicles following terminal depolarization (Bailey et al., 2006). The resulting amplitude of the ST-EPSC is dependent on the quantal content of each vesicle (q) as determined by the average sEPSC amplitude, the number of release sites (N), and the probability of release (P_r) (Bailey et al., 2006; Peters et al., 2008). Data from analysis of the sEPSCs and ST-EPSCs suggest that q, P_r, and N are decreased following vagotomy. However, differentiating between a change in N and P_r is difficult, as decreases in both would be predicted to reduce the average sEPSC frequency and ST-EPSC amplitude, as was observed. To highlight changes in P_r, we delivered a train of stimulations (5 shocks at 50 Hz), and determined that the initial rate of frequency-dependent depression (FDD) is slower at 10 days after vagotomy, consistent with a decrease in initial P_r as a result of the lesion (Fig. 6C). Selective analysis of the paired pulse relationship (PPR) between EPSC 1 and 2 highlights this difference (Fig. 6D). By 60 days post vagotomy, no statistically significant differences in P_r remain ($P = 0.95$).

Progressive increases in stimulation intensity onto the ST can activate additional direct afferent inputs. Convergent inputs are discriminated based on their threshold of activation for each recruited ST-EPSC, latency to ST-EPSC onset, and cumulative amplitude of the multiple ST-EPSCs (i.e., max current change from 1 input alone, 1+2 inputs, 1+2+3 inputs, etc.; Fig. 7) (McDougall et al., 2009; Peters et al., 2011). ST-driven polysynaptic inputs were occasionally recruited and likely contributed modestly to the cumulative amplitude of the compound waveform, but were excluded from the count of monosynaptic ST inputs. By using this incremental stimulus recruitment analysis described above, we were able to functionally map the number of ST afferent inputs that innervate each medial NTS neuron recorded (Fig. 8). In control animals NTS neurons were contacted by at least one ST afferent and the majority received two or more direct inputs (Fig. 8A, left panel). At day 10 post vagotomy over 30% of the recorded NTS neurons received no direct ST afferent innervation (Fig. 8A, right panel, gray bar), consistent with complete withdrawal of the afferent fibers (also described as a complete loss of release sites N). The remaining neurons in this group were innervated by only one or two direct inputs (Fig. 8A, right panel), save the one exception that was contacted by four relatively small inputs (see Fig. 8C for cumulative amplitudes). At day 60 post vagotomy, only 20% now received no afferent innervation, while the overall distribution shifted to the right (greater number of afferent inputs; Fig. 8B, right panel). Even though the number of afferent contacts appears to be recovering at day 60, the cumulative amplitudes of the multiple inputs remain lower than from control animals (Fig. 8D, right panels). Lines connecting points represent the cumulative amplitudes of multiple afferents inputs onto an individual NTS neuron.

DISCUSSION

Vagotomy has been used for decades to determine the contribution of vagal afferents to gastrointestinal physiology (Louis-Sylvestre, 1983). Gastric bypass and related procedures result in de facto selective

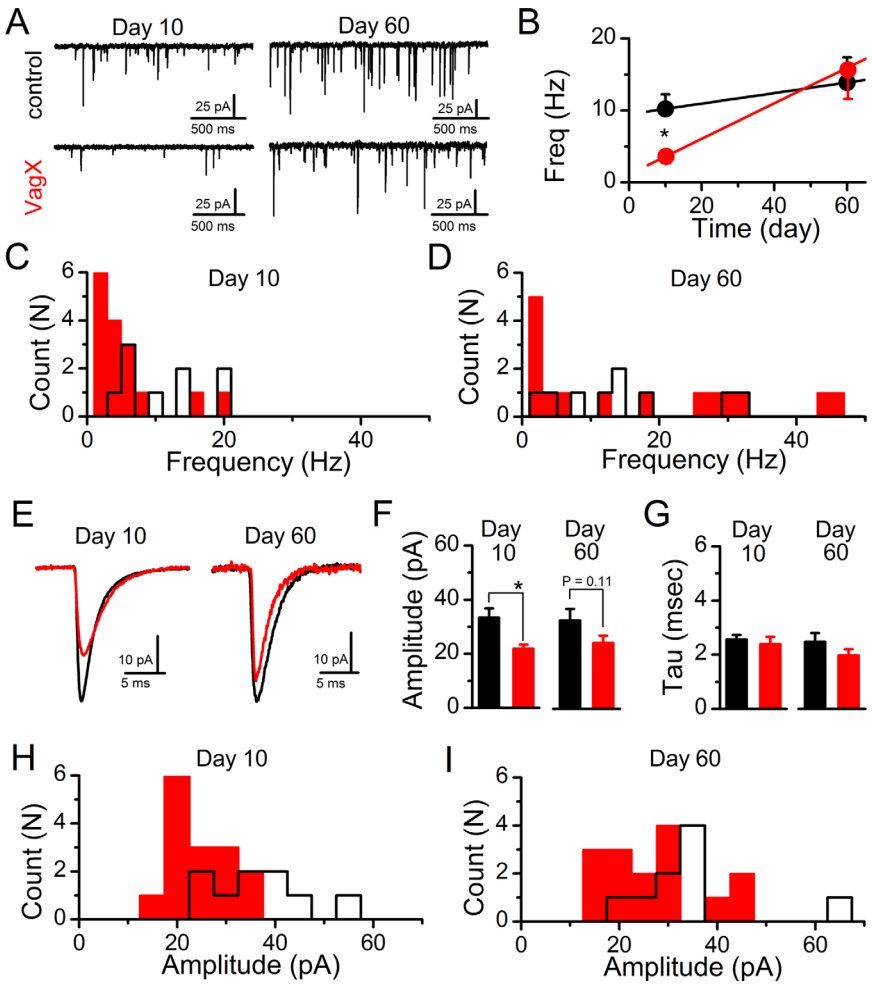

Figure 5. Peripheral vagotomy reversibly decreases the frequency and amplitude of spontaneous glutamate release at central NTS neurons. **A:** Representative traces of sEPSCs onto NTS neurons from control (top) and subdiaphragmatic vagotomized (bottom) animals at 10 and 60 days post surgery. **B:** Across recordings the average frequency of sEPSCs release was slower at 10 days and returned to control levels by 60 days (*P = 0.012). **C,D:** Binned (2-Hz) histograms showing mean sEPSCs frequency across neurons in at 10 (C) and 60 days (D) (control = black/open bars, VagX = red/filled bars). Although neurons receiving low-frequency sEPSCs still occur at 60 days, they were offset by the reemergence of neurons with high-frequency spontaneous inputs. **E:** Representative sEPSC waveforms from control (black) and vagotomized animals (red) at days 10 and 60 post surgery. Traces are the average of 200 sEPSCs. **F:** Vagotomy significantly decreased the average event amplitude at day 10 (*P = 0.012) but not at day 60. **G:** The decay time-constant was unchanged under any condition. **H,I:** Binned (5-pA) histograms showing the mean sEPSC amplitude across neurons under at 10 (H) and 60 days (I) (control = black/open bars, VagX = red/filled bars). The significant decrease in average amplitude was due to an increase in neurons receiving smaller events at day 10. The loss of statistical significance was due to the increased variability in sEPSC amplitude at day 60.

vagotomies, severing anterior and posterior gastric branches of the vagus (Doggrell and Chan, 2012; Cohen et al., 2012). Although the regenerative potential of peripheral nerve trunks is beginning to be established (Phillips et al., 2003; Ryu et al., 2010), the long-term consequences of peripheral nerve damage on central synaptic performance and fiber innervation patterns remain of considerable interest (Gallaher et al., 2011, 2012; Sonoda et al., 2011; Ronchi et al., 2012). This study provides evidence of dynamic synaptic plasticity in the NTS following peripheral nerve damage. We demonstrate that subdiaphragmatic vagotomy produces a dramatic withdrawal of central vagal afferents and weakening of synaptic performance. The extent to which these critical brainstem circuits could be reinnervated was surprising and suggests important implications for both experimental approaches and clinical interventions that involve peripheral vagus nerve damage.

Nerve injuries resulting in axotomy are followed by reinnervation of denervated targets by regeneration of transected axons or collateral sprouting of undamaged axons (Phillips et al., 2003; Ryu et al., 2010). Moreover,

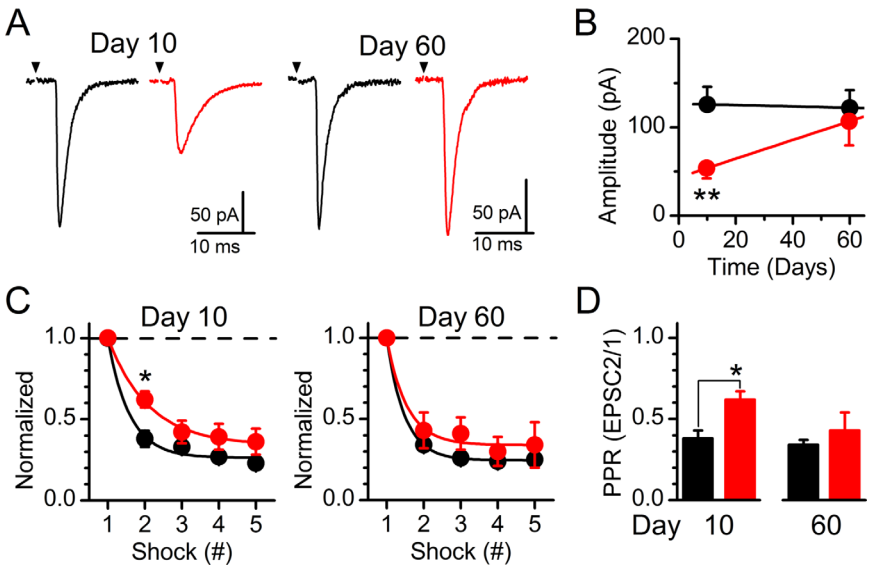

Figure 6. Analysis of solitary tract (ST)-evoked synchronous glutamate release onto NTS neurons. **A:** Average waveform (10 sweeps) of unitary ST-evoked EPSCs from control (black) and vagotomized (red) animals at days 10 and 60 post surgery. **B:** Subdiaphragmatic vagotomy reduced the average amplitude of the first recruited direct ST input at day 10 and was back to control levels by day 60 (**P = 0.007). **C:** Trains of 5 ST shocks (50 Hz) produce frequency-dependent depression of ST-EPSCs. Data are normalized to EPSC1. Inputs from VagX animals had less depression on shock 2 relative to controls on day 10 (*P = 0.01) but not day 60. **D:** Specific examination of the ratio between EPSC 2/1 highlights this reversible change.

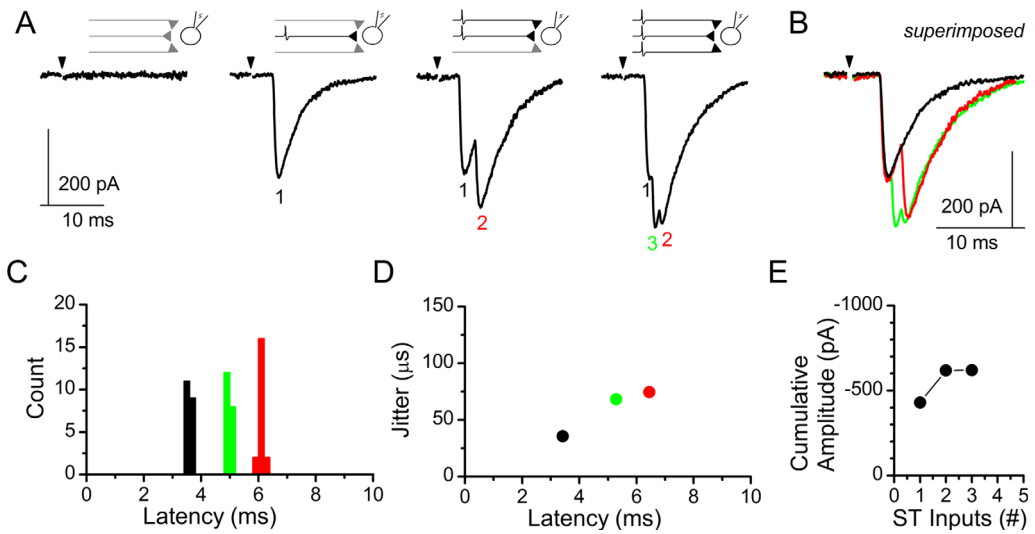

Figure 7. Incremental stimulus recruitment curves allow for differentiation between single and multiple monosynaptic ST-NTS inputs. **A:** Increasing shock intensity recruits individual ST afferent inputs. Low shock intensities are subthreshold for action-potential activation and fail to elicit a postsynaptic ST-EPSC (left panel). ST afferents are activated at precise thresholds in an "all-or-none" response and produce long-latency EPSCs with either simple (second panel from left) or complex (right two panels) waveforms with increasing stimulus intensity, consistent with the progressive recruitment of multiple ST afferents. **B:** Current traces superimposed to show the contribution of each individual afferent contact. The black trace is the first recruited input, the red trace contains inputs 1 and 2, and the green trace is the complex waveform with all three afferent inputs activated. **C,D:** Analysis of (C) event latency (count is ST-EPSCs) and (D) latency versus synaptic "jitter" (standard deviation of the latencies) helps distinguish each input. **E:** Cumulative amplitude of the synaptic current with each recruited synaptic input. The line connects the mean currents for each ST-EPSC onto a single neuron. In this case the neuron is shown in A.

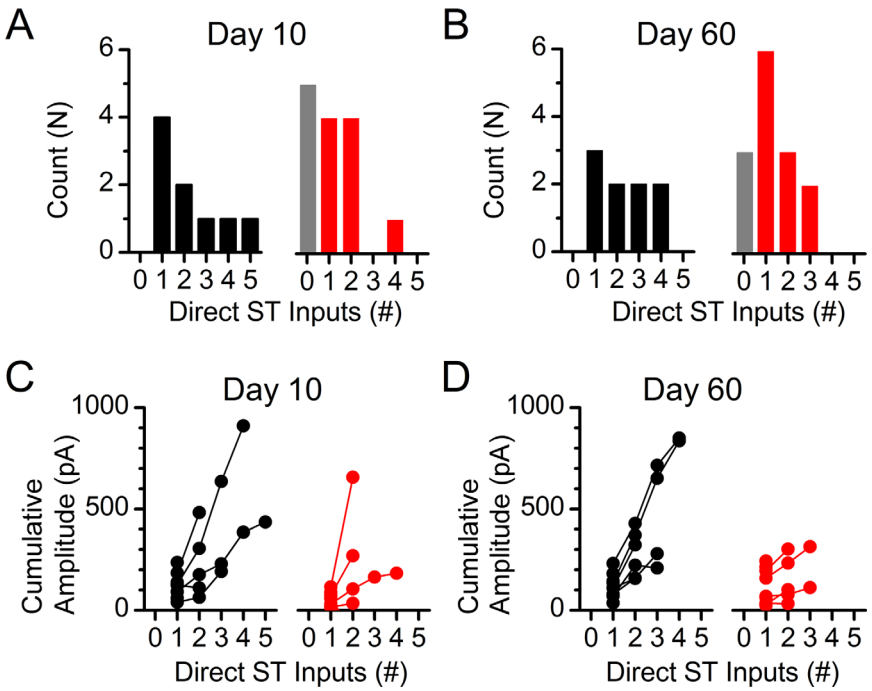

Figure 8. Functional determination of the number of ST–NTS synaptic contacts following subdiaphragmatic vagotomy. **A:** Histogram showing the number of neurons receiving the specified number of direct ST contacts. NTS neurons recorded from control animals always received one or more direct ST contacts, whereas a proportionally large population of neurons recorded from VagX animals received no direct afferent innervation (right panel, gray bar). **B:** By day 60 post vagotomy the number of neurons that received no direct contacts had decreased from 36% (5 of 14 neurons) of the total down to 21% (3 of 14 neurons). **C,D:** Cumulative amplitudes of convergent ST-EPSCs at day 10 (C) and day 60 (D) post vagotomy. Although the occurrence of afferent innervation went up in VagX day 60 recordings, the cumulative amplitude of converging inputs remained attenuated.

there is a retraction of the dendritic tree and a reduction of synapses received by axotomized neurons (Purves, 1975; Tseng and Hu, 1996). Such morphological changes account for a functional isolation of injured neurons from remaining neural circuits and a remodeling of affected CNS areas (Devor and Wall, 1981). Our results expand on previous studies regarding injury-induced plasticity in sensory circuits (Navarro, 2009) and demonstrate that subdiaphragmatic vagotomy triggers transient withdrawal and remodeling of central vagal afferent terminals in the NTS.

Previous studies revealed that vagal afferent innervation of subdiaphragmatic structures, predominantly synapses in the caudal and medial regions of the NTS (Altschuler et al., 1989). Our neural tract-tracing results revealed BDA-labeled vagal afferents across the caudal-to-rostral extent of the NTS, with the highest level of labeling in intermediate regions of the NTS at the level of the area postrema, a consequence of the fact that this particular area contains the greatest cross-sectional area of the NTS (Altschuler et al., 1989). Subdiaphragmatic vagotomy decreased BDA labeling of vagal afferents in the dorsal vagal complex by approximately 70% at 10 days post surgery. In addition, the afferents remaining at 10 days post vagotomy showed significantly weakened synaptic contacts that were represented by a ~50% average reduction in the ST-EPSC amplitude. Thus subdiaphragmatic vagotomy produces a massive withdrawal and synaptic weakening of vagal afferents likely resulting from axon degeneration originating from dying NG neurons or from retraction of axons originating from injured, but surviving NG neurons. The death of ganglionic sensory neurons after axotomy was estimated by previous studies to affect up to 30% of injured neurons (Groves et al., 1997; Vestergaard et al., 1997; Tandrup et al., 2000). Neuronal death had a progressive increase during the first month and then a gradual decline over a period of 6 months (Groves et al., 1997, 1999). Vagotomy was also reported to trigger death of significant populations of neurons in the dorsal motor nucleus of the vagus (Aldskogius and Arvidsson, 1978; Laiwand et al., 1987). Our previous studies revealed that capsaicin-induced damage to vagal viscerosensory afferents triggered

death of approximately 50% of NG neurons over a period of 30 days (Czaja et al., 2008; Gallaher et al., 2011). Functionally, our electrophysiological studies would not be able to discriminate between a loss of innervation due to actual afferent death or simply axonal withdrawal with both appearing as a denervation early in the experimental time-course. The observation that functional afferent reinnervation at day 60 was incomplete is consistent with at least a subpopulation of vagal afferents in the NTS lost due to vagotomy-induced death.

Alternatively, Lancaster et al. (2001) found that vagotomy resulted in a persistent decrease in membrane excitability and failure to maintain action-potential firing following depolarization. This decreased excitability would be predicted to influence the ability to initiate an action potential, especially during trains of stimulations. This decrease in excitability could be contributing to the appearance of NTS neurons now receiving no inputs (Fig. 8). The fact that the decreased excitability persists for more than 20 days would also be consistent with only the partial reversal of the completely dennervated neurons.

However, our longitudinal time-course study demonstrated that decreased BDA labeling of vagal afferents in NTS had recovered to control levels at 30 days and equivalent or higher than control levels by 60 days post vagotomy. These results suggest that a significant population of the damaged NG neurons survived the vagotomy and only temporarily retracted and then reinnervated their central afferents within the NTS. The axotomy-triggered retraction of dendrites was previously shown by multiple studies (Svensson and Aldskogius, 1992; Tseng and Hu, 1996; Nachman-Clewner and Townes-Anderson, 1996). When injured axons are able to regenerate and reinnervate targets, neurons slowly become synaptically functional (Brannstrom and Kellerth, 1999). However, they typically exhibit perikaryon enlargement and dendritic thickening (Bowe et al., 1992). Thickening of central neurites, represented by vagal afferents in NTS, could be responsible for some of the restoration of BDA labeling observed in our study. Because in the NTS the major glutamatergic input is from vagal afferent innervations, changes in sEPSC generally reflect synaptic changes in afferent innervation. Although the presence or absence of the ion channel TRPV1 in the presynaptic afferents is a key determinant of the frequency of spontaneous release, with TRPV1-containing fibers maintaining a higher average rate of release and selectively converging onto NTS neurons (Peters et al., 2010, 2011; Shoudai et al., 2010), our recordings were made in the medial NTS where the majority of neurons receive TRPV1-containing afferent innervation . Thus the time-dependent decrease and then increase in sEPSC frequency is consistent with a loss and then reinnervation by regenerating vagal afferents, rather than a change in TRPV1 expression. Whether the surviving vagal neurons reinnervate the same NTS areas and restore preinjury synaptic connections remains unknown. Alternatively, injury-induced changes in the expression of TRPV1 could account for changes in spontaneous release (Shoudai et al., 2010). However, in primary spinal afferents TRPV1 levels typically rise following injury (Ramer et al., 2012), which would predict an increase in spontaneous release rather than the decrease observed (Fig. 5). Conversely, TRPV1 levels could be decreased; however, the responsiveness to capsaicin in the neurons tested from vagotomized animals was exactly like that of control animals.

Our stereological analysis revealed that the numbers of synapses, but not postsynaptic NTS neurons, were significantly decreased soon after vagotomy. Previous studies show a reduction in number and area of coverage of synaptic terminals on chromatolyzed motoneurons from a few days after axotomy (Svensson et al., 1991). The reduction in number of boutons on the surface membrane is due to the detachment of synapses, which involves disappearance of both pre- and postsynaptic membrane thickenings and a widening of the synaptic cleft (Sumner and Sutherland, 1973; Emirandetti et al., 2010), or synaptic stripping (Tiraihi and Rezaie, 2004; Jinno and Yamada, 2011; Yamada et al., 2011). Consistent with the anatomical findings, the decreased prevalence and strength of direct afferent innervation and the general reduction of spontaneous glutamate release mirror the immunohistochemical data. Recent results suggest that during synaptic remodeling after nerve injury, nitric oxide (NO) acts as a signal for synaptic detachment and inhibits synapse formation (Sunico et al., 2005). Our previously published results also revealed increased NO immunoreactivity in NG neurons after vagotomy, supporting the hypothesis of an injury-induced NO-driven synaptic detachment of central vagal afferents originating in NG and forming the first synapse in NTS (Ryu et al., 2010). The separation of synaptic terminals after injury is also associated with microglia activation (Lan et al., 2003; Gallaher et al., 2012). Loss of presynaptic boutons occurred in parallel with changes in glia activity and appears to be influenced by functional changes in damaged neurons (Chen, 1978; Lan et al., 2003).

The initial vagotomy-induced loss of synapses in the NTS was not permanent and recovered over a period of weeks. Our results show that the number of synapses within the NTS at 60 days post vagotomy did not significantly differ from controls, suggesting that central

vagal synaptic connections were largely restored. Previous results suggest that unilateral cervical vagotomy causes a decrease in synaptic efficacy by both increasing the overall percentage of synaptic failures and shifting the population of NTS synapses toward a more high failure transmission (Swartz and Weinreich, 2009). This study combined recordings from across animals 6–30 days post vagotomy, a time period we now appreciate exhibits dynamic changes in afferent death and synaptic withdrawal/reinnervation. Our results are consistent with this report in that synaptic strength is diminished primarily via a decrease in a presynaptic release probability although we did not observe the dramatic increase in failures. This was likely because we unintentionally masked this effect by increasing the release probability through recording in a 2-mM bath calcium, whereas Swartz and Weinreich (2009) recorded in a 1-mM bath calcium. Furthermore, our lesion targeted the subdiaphragmatic abdominal afferents, which provide a dominant innervation into the medial NTS, resulting in a somewhat less "traumatic" injury. Even considering this discrete lesion, we found that in contrast with this previous work, we report statistically lower frequencies of sEPSCs following vagotomy, smaller sEPSC and unitary evoked EPSC amplitudes, and increased proportion of neurons that received no direct afferent innervation following vagotomy, conditions that resolved toward control levels by 60 days. This restoration in central synapses may be due to the return of retracted central terminals from injured but surviving NG neurons or the sprouting of uninjured afferent axons and intrinsic NTS neurons, which may contribute to the increase in the number of NTS synapses. The fact that some NTS neurons received very high frequencies of sEPSCs at 60 days post vagotomy may indicate compensatory sprouting. Axotomy-induced alterations in the number of central synapses were also reported in the spinal innervation (White and Kocsis, 2002; Sun et al., 2006) and cortex (Kim and Nabekura, 2011). Initial losses of the central synaptic connections were also shown to be eventually restored when the reinnervation of the peripheral target organs was completed (Brannstrom and Kellerth, 1999).

Our study shows that damage to peripheral axons of the vagus induces reorganization of central vagal afferents and synaptic plasticity in the NTS. Moreover, subdiaphragmatic vagotomy results in transient decrease in the density of vagal afferents projecting to the NTS and alters both the number and functioning of synapses. Our results increase the understanding of injury-induced plasticity of central vagal afferents in relation to its potential effects on autonomic reflex pathways, the control of food intake, and energy homeostasis.

CONFLICT OF INTEREST STATEMENT

The authors declare no conflict of interest.

ROLE OF AUTHORS

All authors had full access to all the data in the study and take responsibility for the integrity of the data and the accuracy of the data analysis. Study concept and design: J.H.P. and K.C. Acquisition of data: J.H.P., Z.R.G., V.R., and K.C. Analysis and interpretation of data: J.H.P. and K.C. Drafting of the article: J.H.P. and K.C. Critical revision of the article for important intellectual content: J.H.P. and K.C. Obtained funding: J.H.P. and K.C. Study supervision: K.C.

LITERATURE CITED

Aldskogius H, Arvidsson J. 1978. Nerve cell degeneration and death in the trigeminal ganglion of the adult rat following peripheral nerve transection. J Neurocytol 7:229–250.

Altschuler SM, Bao XM, Bieger D, Hopkins DA, Miselis RR. 1989. Viscerotopic representation of the upper alimentary tract in the rat: sensory ganglia and nuclei of the solitary and spinal trigeminal tracts. J Comp Neurol 283: 248–268.

Andresen MC, Mendelowitz D. 1996. Sensory afferent neurotransmission in caudal nucleus tractus solitarius–common denominators. Chem Senses 21:387–395.

Bailey TW, Jin YH, Doyle MW, Smith SM, Andresen MC. 2006. Vasopressin inhibits glutamate release via two distinct modes in the brainstem. J Neurosci 26:6131–6142.

Bailey TW, Appleyard SM, Jin YH, Andresen MC. 2008. Organization and properties of GABAergic neurons in solitary tract nucleus (NTS). J Neurophysiol 99:1712–1722.

Berthoud HR, Shin AC, Zheng H. 2011. Obesity surgery and gut-brain communication. Physiol Behav 105:106–119.

Bowe CM, Evans NH, Vlacha V. 1992. Progressive morphological abnormalities observed in rat spinal motor neurons at extended intervals after axonal regeneration. J Comp Neurol 321:576–590.

Brannstrom T, Kellerth JO. 1999. Recovery of synapses in axotomized adult cat spinal motoneurons after reinnervation into muscle. Exp Brain Res 125:19–27.

Calhoun ME, Jucker M, Martin LJ, Thinakaran G, Price DL, Mouton PR. 1996. Comparative evaluation of synaptophysin-based methods for quantification of synapses. J Neurocytol 25:821–828.

Chen DH. 1978. Qualitative and quantitative study of synaptic displacement in chromatolyzed spinal motoneurons of the cat. J Comp Neurol 177:635–664.

Cohen RV, Pinheiro JC, Schiavon CA, Salles JE, Wajchenberg BL, Cummings DE. 2012. Effects of gastric bypass surgery in patients with type 2 diabetes and only mild obesity. Diabetes Care 35:1420–1428.

Czaja K, Burns GA, Ritter RC. 2008. Capsaicin-induced neuronal death and proliferation of the primary sensory neurons located in the nodose ganglia of adult rats. Neuroscience 154:621–630.

Devor M, Wall PD. 1981. Plasticity in the spinal cord sensory map following peripheral nerve injury in rats. J Neurosci 1:679–684.

Doggrell SA, Chan V. 2012. Bariatric surgery or medicine for type 2 diabetes? Expert Opin Pharmacother 13:2249–2253.

Doyle MW, Andresen MC. 2001. Reliability of monosynaptic sensory transmission in brain stem neurons in vitro. J Neurophysiol 85:2213–2223.

Doyle MW, Bailey TW, Jin YH, Appleyard SM, Low MJ, Andresen MC. 2004. Strategies for cellular identification in nucleus tractus solitarius slices. J Neurosci Methods 137:37–48.

Emirandetti A, Simoes GF, Zanon RG, Oliveira AL. 2010. Spinal motoneuron synaptic plasticity after axotomy in the absence of inducible nitric oxide synthase. J Neuroinflammation 7:31.

Furness JB, Kunze WA, Clerc N. 1999. Nutrient tasting and signaling mechanisms in the gut. II. The intestine as a sensory organ: neural, endocrine, and immune responses. Am J Physiol 277:G922–G928.

Gallaher ZR, Ryu V, Larios RM, Sprunger LK, Czaja K. 2011. Neural proliferation and restoration of neurochemical phenotypes and compromised functions following capsaicin-induced neuronal damage in the nodose ganglion of the adult rat. Front Neurosci 5:12.

Gallaher ZR, Ryu V, Herzog T, Ritter RC, Czaja K. 2012. Changes in microglial activation within the hindbrain, nodose ganglia, and the spinal cord following subdiaphragmatic vagotomy. Neurosci Lett 513:31–36.

Gazula VR, Strumbos JG, Mei X, Chen H, Rahner C, Kaczmarek LK. 2010. Localization of Kv1.3 channels in presynaptic terminals of brainstem auditory neurons. J Comp Neurol 518:3205–3220.

Groves MJ, Christopherson T, Giometto B, Scaravilli F. 1997. Axotomy-induced apoptosis in adult rat primary sensory neurons. J Neurocytol 26:615–624.

Groves MJ, An SF, Giometto B, Scaravilli F. 1999. Inhibition of sensory neuron apoptosis and prevention of loss by NT-3 administration following axotomy. Exp Neurol 155:284–294.

Herde MK, Friauf E, Rust MB. 2010. Developmental expression of the actin depolymerizing factor ADF in the mouse inner ear and spiral ganglia. J Comp Neurol 518:1724–1741.

Hu J, Mata M, Hao S, Zhang G, Fink DJ. 2004. Central sprouting of uninjured small fiber afferents in the adult rat spinal cord following spinal nerve ligation. Eur J Neurosci 20:1705–1712.

Hunter DA, Moradzadeh A, Whitlock EL, Brenner MJ, Myckatyn TM, Wei CH, Tung TH, Mackinnon SE. 2007. Binary imaging analysis for comprehensive quantitative histomorphometry of peripheral nerve. J Neurosci Methods 166: 116–124.

Jinno S, Yamada J. 2011. Using comparative anatomy in the axotomy model to identify distinct roles for microglia and astrocytes in synaptic stripping. Neuron Glia Biol 7:55–66.

Kavalali ET, Chung C, Khvotchev M, Leitz J, Nosyreva E, Raingo J, Ramirez DM. 2011. Spontaneous neurotransmission: an independent pathway for neuronal signaling? Physiology (Bethesda) 26:45–53.

Kim SK, Nabekura J. 2011. Rapid synaptic remodeling in the adult somatosensory cortex following peripheral nerve injury and its association with neuropathic pain. J Neurosci 31:5477–5482.

Laiwand R, Werman R, Yarom Y. 1987. Time course and distribution of motoneuronal loss in the dorsal motor vagal nucleus of guinea pig after cervical vagotomy. J Comp Neurol 256:527–537.

Lan CT, Hsu JC, Chang CN, Chuang HL, Ling EA. 2003. Synaptic remodeling in the dorsal motor nucleus of the vagus nerve following vagal-hypoglossal nerve anastomosis in the cat. J Comp Neurol 458:195–207.

Lancaster E, Oh EJ, Weinreich D. 2001. Vagotomy decreases excitability in primary vagal afferent somata. J Neurophysiol 85:247–253.

Li Y, Owyang C. 2003. Musings on the wanderer: what's new in our understanding of vago-vagal reflexes? V. Remodeling of vagus and enteric neural circuitry after vagal injury. Am J Physiol Gastrointest Liver Physiol 285:G461–G469.

Louis-Sylvestre J. 1983. Validation of tests of completeness of vagotomy in rats. J Auton Nerv Syst 9:301–314.

McDougall SJ, Peters JH, Andresen MC. 2009. Convergence of cranial visceral afferents within the solitary tract nucleus. J Neurosci 29:12886–12895.

Micheva KD, Busse B, Weiler NC, O'Rourke N, Smith SJ. 2010. Single-synapse analysis of a diverse synapse population: proteomic imaging methods and markers. Neuron 68:639–653.

Nachman-Clewner M, Townes-Anderson E. 1996. Injury-induced remodelling and regeneration of the ribbon presynaptic terminal in vitro. J Neurocytol 25:597–613.

Navarro X. 2009. Chapter 27 neural plasticity after nerve injury and regeneration. Int Rev Neurobiol 87:483–505.

Navarro X, Vivo M, Valero-Cabre A. 2007. Neural plasticity after peripheral nerve injury and regeneration. Prog Neurobiol 82:163–201.

Peters JH, McDougall SJ, Kellett DO, Jordan D, Llewellyn-Smith IJ, Andresen MC. 2008. Oxytocin enhances cranial visceral afferent synaptic transmission to the solitary tract nucleus. J Neurosci 28:11731–11740.

Peters JH, McDougall SJ, Fawley JA, Smith SM, Andresen MC. 2010. Primary afferent activation of thermosensitive TRPV1 triggers asynchronous glutamate release at central neurons. Neuron 65:657–669.

Peters JH, McDougall SJ, Fawley JA, Andresen MC. 2011. TRPV1 marks synaptic segregation of multiple convergent afferents at the rat medial solitary tract nucleus. PLoS ONE 6:e25015.

Phillips RJ, Powley TL. 2005. Plasticity of vagal afferents at the site of an incision in the wall of the stomach. Auton Neurosci 123:44–53.

Phillips RJ, Baronowsky EA, Powley TL. 2000. Regenerating vagal afferents reinnervate gastrointestinal tract smooth muscle of the rat. J Comp Neurol 421:325–346.

Phillips RJ, Baronowsky EA, Powley TL. 2003. Long-term regeneration of abdominal vagus: efferents fail while afferents succeed. J Comp Neurol 455:222–237.

Powley TL, Fox EA, Berthoud HR. 1987. Retrograde tracer technique for assessment of selective and total subdiaphragmatic vagotomies. Am J Physiol 253:R361–R370.

Purves D. 1975. Functional and structural changes in mammalian sympathetic neurones following interruption of their axons. J Physiol 252:429–463.

Ramer LM, van Stolk AP, Inskip JA, Ramer MS, Krassioukov AV. 2012. Plasticity of TRPV1-expressing sensory neurons mediating autonomic dysreflexia following spinal cord injury. Front Physiol 3:257.

Ronchi G, Ryu V, Fornaro M, Czaja K. 2012. Hippocampal plasticity after a vagus nerve injury in the rat. Neural Regen Res 7:1055–1063.

Ryu V, Gallaher Z, Czaja K. 2010. Plasticity of nodose ganglion neurons after capsaicin- and vagotomy-induced nerve damage in adult rats. Neuroscience 167:1227–1238.

Schwartz GJ. 2006. Integrative capacity of the caudal brainstem in the control of food intake. Philos Trans R Soc Lond B Biol Sci 361:1275–1280.

Shoudai K, Peters JH, McDougall SJ, Fawley JA, Andresen MC. 2010. Thermally active TRPV1 tonically drives central spontaneous glutamate release. J Neurosci 30:14470–14475.

Soiza-Reilly M, Commons KG. 2011. Quantitative analysis of glutamatergic innervation of the mouse dorsal raphe nucleus using array tomography. J Comp Neurol 519: 3802–3814.

Sonoda EY, Gomes da SS, Arida RM, Giglio PN, Margarido NF, Martinez CA, Pansani AP, Maciel RS, Cavalheiro EA, Scorza FA. 2011. Hippocampal plasticity in rats submitted to a gastric restrictive procedure. Nutr Neurosci 14: 181–185.

Sumner BE, Sutherland FI. 1973. Quantitative electron microscopy on the injured hypoglossal nucleus in the rat. J Neurocytol 2:315–328.

Sun T, Xiao HS, Zhou PB, Lu YJ, Bao L, Zhang X. 2006. Differential expression of synaptoporin and synaptophysin in primary sensory neurons and up-regulation of synaptoporin after peripheral nerve injury. Neuroscience 141:1233–1245.

Sunico CR, Portillo F, Gonzalez-Forero D, Moreno-Lopez B. 2005. Nitric-oxide-directed synaptic remodeling in the adult mammal CNS. J Neurosci 25:1448–1458.

Svensson M, Aldskogius H. 1992. The effect of axon injury on microtubule-associated proteins MAP2, 3 and 5 in the hypoglossal nucleus of the adult rat. J Neurocytol 21:222–231.

Svensson M, Tornqvist E, Aldskogius H, Cova JL. 1991. Synaptic detachment from hypoglossal neurons after different types of nerve injury in the cat. J Hirnforsch 32:547–552.

Swartz JB, Weinreich D. 2009. Influence of vagotomy on monosynaptic transmission at second-order nucleus tractus solitarius synapses. J Neurophysiol 102:2846–2855.

Tandrup T, Woolf CJ, Coggeshall RE. 2000. Delayed loss of small dorsal root ganglion cells after transection of the rat sciatic nerve. J Comp Neurol 422:172–180.

Tiraihi T, Rezaie MJ. 2004. Synaptic lesions and synaptophysin distribution change in spinal motoneurons at early stages following sciatic nerve transection in neonatal rats. Brain Res Dev Brain Res 148:97–103.

Tseng GF, Hu ME. 1996. Axotomy induces retraction of the dendritic arbor of adult rat rubrospinal neurons. Acta Anat (Basel) 155:184–193.

Vestergaard S, Tandrup T, Jakobsen J. 1997. Effect of permanent axotomy on number and volume of dorsal root ganglion cell bodies. J Comp Neurol 388:307–312.

White FA, Kocsis JD. 2002. A-fiber sprouting in spinal cord dorsal horn is attenuated by proximal nerve stump encapsulation. Exp Neurol 177:385–395.

Wimmer VC, Horstmann H, Groh A, Kuner T. 2006. Donut-like topology of synaptic vesicles with a central cluster of mitochondria wrapped into membrane protrusions: a novel structure-function module of the adult calyx of Held. J Neurosci 26:109–116.

Yamada J, Nakanishi H, Jinno S. 2011. Differential involvement of perineuronal astrocytes and microglia in synaptic stripping after hypoglossal axotomy. Neuroscience 182:1–10.